Flow Electrochemistry Hot Paper

International Edition: DOI: 10.1002/anie.201709717
German Edition: DOI: 10.1002/ange.201709717

An Easy-to-Machine Electrochemical Flow Microreactor: Efficient Synthesis of Isoindolinone and Flow Functionalization

*Ana A. Folgueiras-Amador, Kai Philipps, Sébastien Guilbaud, Jarno Poelakker, and Thomas Wirth**

Abstract: *Flow electrochemistry is an efficient methodology to generate radical intermediates. An electrochemical flow microreactor has been designed and manufactured to improve the efficiency of electrochemical flow reactions. With this device only little or no supporting electrolytes are needed, making processes less costly and enabling easier purification. This is demonstrated by the facile synthesis of amidyl radicals used in intramolecular hydroaminations to produce isoindolinones. The combination with inline mass spectrometry facilitates a much easier combination of chemical steps in a single flow process.*

Over the past decades, organic electrosynthesis has become recognized as one of the methodologies to perform redox reactions in an efficient, straightforward, and clean way. Anionic and cationic radical species can be formed from neutral organic molecules generating a wide variety of useful reactive intermediates.[1] Electrons as reagents can achieve oxidations and reductions by replacing toxic or dangerous oxidizing or reducing reagents. As smaller amounts of chemicals are necessary for these reactions, fewer side products are formed. These features have recently sparked interest in the development of equipment[2] and in advanced synthetic protocols for electrochemical reactions.[3]

Organic electrochemistry is a powerful method for organic synthesis, but there are also limitations for electrochemistry in batch processes. As common organic solvents have typically low conductivity, the use and subsequent removal of supporting electrolytes is necessary. The large distance between electrodes in batch processes leads to large current gradients. Continuous flow reactors can address some of these problems.[4] Small electrode distances avoid large current gradients and reactions can be performed with small amounts or even without addition of supporting electrolytes, although modification of electrode surfaces has also been investigated.[5] A high electrode surface-to-reactor volume ratio allows a much improved mass transfer on the surface of the electrodes leading to milder reaction conditions and short reaction times.

Microreactors for continuous flow electrosynthesis have already been developed.[6] We have contributed to this development with an electrochemical microreactor having a very small inter-electrode gap (100–250 μm), which was applied for the synthesis of diaryl iodonium salts, for the difluoro- and trifluoromethylation of electron-deficient alkenes, and for the electrochemical deprotection of the *iso*-nicotinyloxycarbonyl group on carbonates and thiocarbonates.[7] Here we describe the development of a much improved, second-generation electrochemical microreactor. This reactor can be made with an aluminum body (Figure 1 b), or from polymers by using additive manufacturing technology (3D printing, Figure 1 c). The latter offers the possibility for the reactor to be manufactured at lower cost within a few hours and also offers facile customization if needed according to the specifications of the reaction. The large electrode area (anode and cathode: 25 cm^2 each) with robust and secure electrode–wire connection and easily exchangeable electrode materials leads to more flexibility as well as higher productivity and efficiency. The two electrodes are separated by a FEP (fluorinated ethylene propylene) film spacer, while the reaction solution flows through a channel cut into the FEP film (Figure 1 d). The FEP spacer serves as a seal when the two electrode blocks are screwed together. The flow reactor is shown in Figure 1 and all details of its construction including files for additive manufacturing (3D printing) can be found in

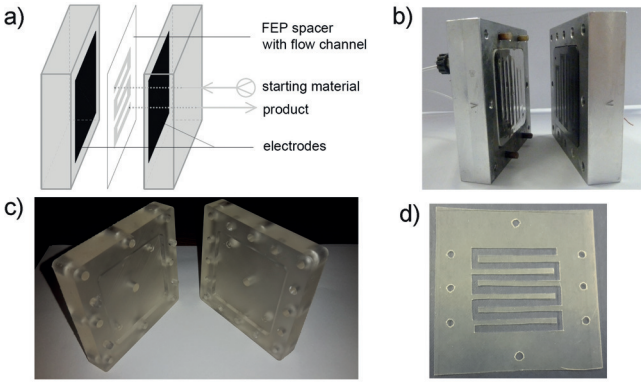

Figure 1. Electrochemical flow reactor. a) Schematic diagram; b) aluminum reactor; c) reactor made by additive manufacturing through monomer polymerization; d) FEP spacer with flow channel.

[*] A. A. Folgueiras-Amador, K. Philipps, S. Guilbaud, J. Poelakker, Prof. Dr. T. Wirth
School of Chemistry, Cardiff University
Park Place, Main Building, Cardiff CF10 3AT (UK)
E-mail: wirth@cf.ac.uk
Homepage: http://blogs.cardiff.ac.uk/wirth/

Supporting information and the ORCID identification number(s) for the author(s) of this article can be found under: https://doi.org/10.1002/anie.201709717.

the Supporting Information. The distance between the electrodes is defined by the thickness of the FEP film (typically 100–500 μm). A small distance between the electrodes is important and the use of supporting electrolytes often superfluous.

Nitrogen-containing heterocycles are very important components in drugs and bioactive natural products. Their synthesis has been explored with different methodologies, many of them involving the use of precious transition metals or toxic reagents.[8] Using the above-described electrochemical flow reactor, we applied an alternative method for the synthesis of N-heterocycles via a nitrogen-centered radical accessed through electrochemical oxidation and its subsequent addition to alkenes in an intramolecular cyclization. Such N-centered radicals have already been used in batch electrochemical processes.[9]

We focussed on the cyclization of carbamate **1** to product **2** (Scheme 1), and general conditions for the electrochemical reaction were explored such as electrode materials, solvents, and bases. In batch reactions, where NBu_4BF_4 (0.1 M) is used as the supporting electrolyte, different electrode materials were investigated to explore the reactivity.

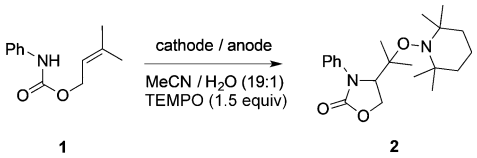

1 2

Scheme 1. Electrochemical cyclization of carbamate **1**. TEMPO = 2,2,6,6-tetramethylpiperidinyloxyl.

With platinum as the cathode, the reaction behaved very similarly when almost any electrode material was used as anode. But the results are very different when the cathode is not platinum. In theory, only 1 F mol^{-1} of electricity is necessary for the one-electron oxidation, but even with 4 F mol^{-1} the reaction did not go to completion in most cases (see the Supporting Information for details). The counter electrode (cathode) clearly has a larger impact on the reaction than the working electrode (anode). This is due to the water reduction reaction taking place at the cathode (see the proposed mechanism in Scheme 2), and the different activation overpotential for hydrogen evolution on different electrode materials.[10] The activation overpotential is lower for platinum (−0.07 V) than for nickel (−0.28 V), and much higher for graphite (−0.62 V) (all vs. standard hydrogen electrode). As the results obtained for graphite, platinum, and boron-doped diamond (BDD) as the anode are very similar, graphite was used since it is the least expensive material.

The reaction from **1** to **2** was carried out in different solvents and solvent mixtures, such as acetonitrile, methanol, 1,1,1,3,3,3-hexafluoroisopropyl alcohol (HFIP), and water, and it was found that acetonitrile/water mixture is the optimum solvent mixture for this reaction. Although HFIP is known to be efficient for stabilizing cations and radicals,[11] this solvent led to either recovery of starting material (< 2 F mol^{-1}) or decomposition (> 3 F mol^{-1}).

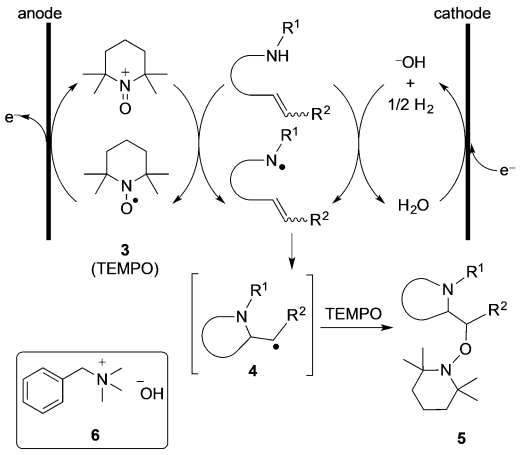

Scheme 2. Proposed mechanism.[9]

The use of a base can be favorable in anodic oxidations if the compound or its oxidized form can be deprotonated, because most anodic oxidations proceed by loss of electrons and protons.[9b,12] Xu et al.[9] reported the batch cyclization of carbamates of type **1** using lithium hydroxide or sodium carbonate as a heterogeneous base. The drawback of these bases is their low solubility in organic solvents which is clearly more problematic for flow than for batch processes. Different organic bases were investigated in the flow cyclizations (see the Supporting Information), but triethylamine inhibited the reaction while with 2,6-lutidine conversions similar to those without base were observed. This was explained by measuring the cyclic voltammogram of substrate **1** in the presence of different bases (see the Supporting Information). The oxidation potential of triethylamine is much lower than of **1**, so it will be oxidized first, and the starting material remains unreacted. The oxidation potential of **1** after addition of 2,6-lutidine remains practically unchanged, which explains the similar result with and without base.

The mechanism proposed by Xu et al.[9] (Scheme 2) shows that the cathode-generated hydroxide anion assists in the deprotonation of the carbamate before forming the nitrogen radical. With sodium carbonate as base the reaction proceeded to completion after 3 F mol^{-1}, but the amount of water had to be increased (to 50 % in acetonitrile) in order to dissolve the base. This led to poor solubility of the product in the solvent mixture and to precipitation and blocking of the flow system after 10 minutes of operation, making this base/solvent system inefficient for continuous flow.

To accelerate the reaction, benzyltrimethylammonium hydroxide **6** was used. Full conversion of **1** after 3 F mol^{-1} was achieved and **6** as a soluble base was used in further optimization studies. Cyclic voltammetry endorses this result, as the cyclic voltammogram in the presence of benzyltrimethylammonium hydroxide shows a lower oxidation potential (from 1.74 V to 0.27 V, vs. Ag/AgCl). This second oxidation potential corresponds to the deprotonated form of compound **1**, which will facilitate the production of the radical at the anode (see the Supporting Information). Moeller and co-workers have observed comparable results where deprotonated sulfonamides exhibit a lower oxidation

potential than the neutral compounds.[13] We also found that under the optimized reaction conditions the thickness of the spacer can be varied from 250 μm to 500 μm with no change in the reaction yield.

The optimized conditions were then applied to the synthesis of isoindolinones in flow. Such isoindolinone motifs are found in many natural products, pharmaceuticals, and biologically active molecules (Figure 2).[14]

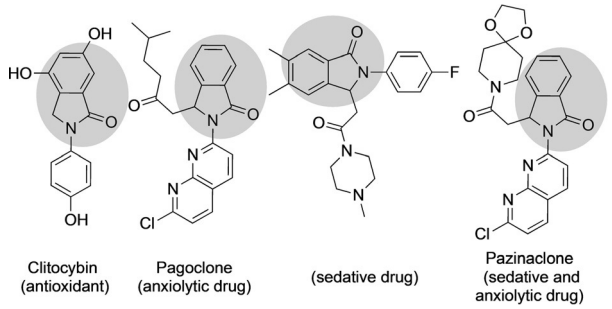

Figure 2. Biologically active isoindolinone derivatives.

The cyclization of amide **7** to isoindolinone **8** was investigated in detail (Scheme 3). For this purpose, the electrochemical reactor was connected to an inline mass spectrometer, which allowed a rapid assessment of the required amount of electrons. As shown in Figure 3, at least 3 F mol^{-1} is necessary in order to achieve full conversion. Only 0.5 equiv of the base is needed to complete the reaction, but with a smaller amount of base full conversion cannot be achieved. Here the base can be considered as a supporting electrolyte, but with much lower loadings than the supporting electrolytes in batch electrochemical reactions, and the base can be removed easily through aqueous work-up.

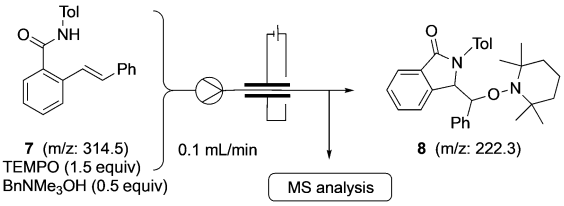

Scheme 3. Cyclization of amide **7** to **8** with MS analysis. Bn = benzyl, Tol = tolyl.

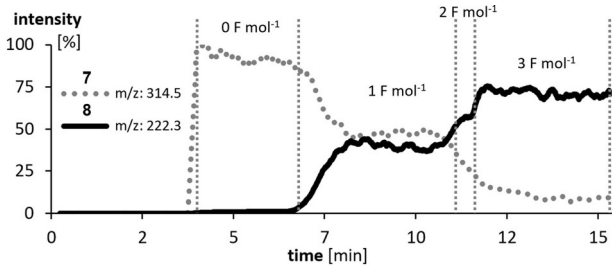

Figure 3. Inline mass spectrometric analysis of the electrochemical flow reaction **7**→**8**.

With the optimized reaction conditions in hand (3 F mol^{-1}, 24 mA, 1–2 V), we examined different substrates as shown in Figure 4. While aromatic moieties on the amide nitrogen are required to stabilize the nitrogen radical, the substituents on the alkene moiety can be varied widely.

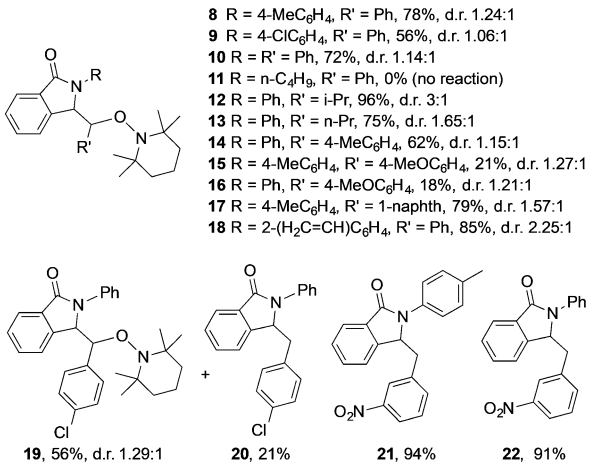

Figure 4. Substrate scope for the cyclization reaction.

Only with the substrate in which the 4-OMe functionality is present in the aromatic ring next to the double bond, the reaction results in a complex mixture leading to a low yield of the desired products (**15** and **16**). Due to the radical pathway of the cyclization, the diastereoselectivities are low and were dictated only by steric effects. The stereochemistry of the substrate was also found not to affect the selectivity. Thus when pure *E*- or *Z*-isomers are used for the reaction the same diastereomeric ratios are obtained for compound **12**. The (*R*,*S*)/(*S*,*R*) diastereomer is always favored as confirmed by X-ray crystallographic analysis of compound **12** (see the Supporting Information).[15] When electron-withdrawing substituents such as chloride are attached to the aromatic ring adjacent to the double bond, the reduced product **20** is observed in addition to **19**. Such reduced compounds are the only products with a 3-nitrophenyl substituent (**21** and **22**), where no TEMPO addition is observed. In these reactions no gas evolution is observed, which implies that there is no gaseous hydrogen formed from proton reduction. TEMPO is not being consumed here, since it does not add to the final product. Thus, the redox cycle can be completed by reduction of the oxoammonium cation to the free radical.

A flow reaction on slightly larger scale was performed for 1.5 h leading to **12** in 96% yield (180 mg). The same reaction performed in a batch format required supporting electrolyte and provided product **12** after 6 h in only 51% yield (107 mg). This also demonstrates the efficiency of the flow process, allowing a supporting electrolyte-free electrochemical reaction.

A tandem cyclization reaction was then attempted with a substrate having a vinylphenyl substituent on the nitrogen, but only the monocyclized product **18** was obtained (Scheme 4). This compound bears a functionalized styrene moiety which could be used in subsequent reactions. NMR

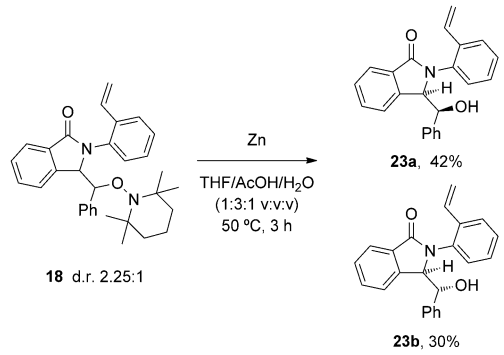

Scheme 4. N–O-bond cleavage of compound **18**.

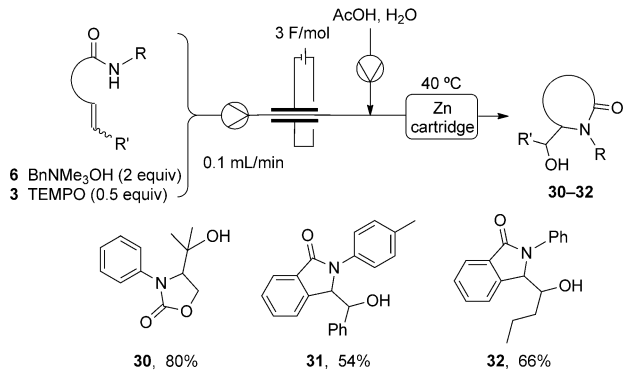

Scheme 6. Two-step flow reaction: cyclization and reduction.

characterization of **18** was difficult due to the appearance of broad peaks, which could only be slightly improved at high temperature. After separation of the diastereomers, the oxygen–nitrogen bond was cleaved with zinc and acetic acid and the structures of the two diastereoisomers **23a** and **23b** were determined by X-ray analysis (see the Supporting Information).[15]

The isoindolinone products were then used for subsequent functionalization, including elimination of the TEMPO moiety and reduction of the nitrogen–oxygen bond. The elimination reaction was performed using the same base as that used in the cyclization to yield alkenes such as **24**,[16] which can be employed in further reactions. Furthermore, the electrochemical cyclization and the elimination were coupled in a single flow system as shown in Scheme 5.

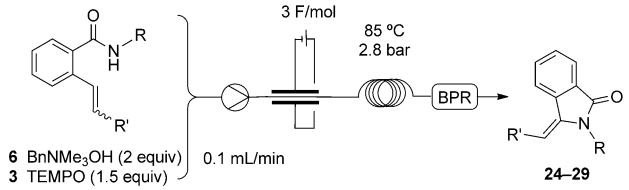

24 R = Ph, R' = i-Pr, 75%, E/Z : 9/1
25 R = 4-MeC$_6$H$_4$, R' = Ph, 68%, E/Z : 19/1
26 R = R' = Ph, 62%, E/Z : 19/1
27 R = Ph, R' = 4-MeC$_6$H$_4$, 71%, E/Z : 9/1
28 R = Ph, R' = 4-ClC$_6$H$_4$, 73%, E/Z : 7/1
29 R = 4-ClC$_6$H$_4$, R' = Ph, 66%, E/Z : 5/1

Scheme 5. Two-step flow reaction: cyclization and elimination. BPR: backpressure regulator.

In order to achieve full conversion to compound **24**, the reaction conditions were investigated and a residence time of 25 minutes at 85 °C/ 2.8 bar was found to be optimal (see the Supporting Information, Table S2). Compound **24** was obtained as a mixture of *E*- and *Z*-isomers, with an excess of the *E*-isomer (up to 9:1 in entry 6 for compound **24**, and up to 19:1 for compounds **25** and **26**). The configuration was determined by NOE NMR spectroscopy (see the Supporting Information).

Reduction of the nitrogen–oxygen bond under flow conditions was performed using a Zn cartridge[17] and acetic acid, as shown in Scheme 6.[18] The cartridge was heated to 40 °C to achieve full conversion to the corresponding alcohols (Scheme 6). Compounds **30–32** were prepared in 54–80 % overall yield.

Two additional transformations performed in the electrochemical flow reactor without supporting electrolyte are shown in Scheme 7. The electrolysis of thioacetic acid

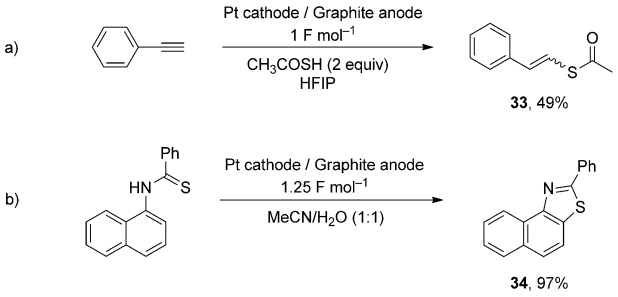

Scheme 7. a) Electrochemical addition of thioacetic acid to phenyl acetylene; b) electrochemical C–H thiolation of an *N*-arylthioamide to benzothiazole **34**.

generates the corresponding radical. Unlike carboxylic acids, which decarboxylate and react in Kolbe reactions, the thioacetyl radical is stable and adds smoothly to terminal alkynes to yield products such as **33**. The use of hexafluoroisopropanol (HFIP) to stabilize the formed radical is crucial, as with other solvents dimerization of thioacetic acid is observed. An intramolecular C–H thiolation of *N*-arylthioamides to form benzothiazoles such as **34** can also be performed with superior yields than with the batch process, which requires TEMPO and a supporting electrolyte to operate.[19]

In conclusion, a new and efficient electrochemical flow microreactor has been designed and manufactured which was used to generate nitrogen- and sulfur-based radical intermediates for syntheses with no or little supporting electrolyte. In addition, one of the first combinations of an electrochemical reaction with another reaction in a single flow system is demonstrated.[20]

Acknowledgements

We thank the workshop staff from Cardiff School of Chemistry for helping in manufacturing the reactor and Prof. S. Waldvogel, Mainz University, for facilitating the electrode and solvent screening in his laboratory. We thank Dr. D. L. Browne, Cardiff University, for helpful discussions and S. Cattaneo, CCI at Cardiff University, for assistance with the 3D printing. We also thank the EPSRC National Mass Spectrometry Facility, Swansea, for mass spectrometric data. We thank Cardiff University and the Erasmus program (K.P.) for financial support.

Conflict of interest

The authors declare no conflict of interest.

Keywords: cyclizations · flow electrochemistry · isoindolinones · microreactors · tandem reactions

How to cite: *Angew. Chem. Int. Ed.* **2017**, *56*, 15446–15450
Angew. Chem. **2017**, *129*, 15648–15653

[1] a) B. A. Frontana-Uribe, R. D. Little, J. G. Ibanez, A. Palma, R. Vasquez-Medrano, *Green Chem.* **2010**, *12*, 2099–2119; b) O. Hammerich, B. Speiser, *Organic Electrochemistry*, CRC Press, Boca Raton, **2016**; c) E. J. Horn, B. R. Rosen, P. S. Baran, *ACS Cent. Sci.* **2016**, *2*, 302–308.

[2] M. Yan, Y. Kawamata, P. S. Baran, *Angew. Chem. Int. Ed.* **2017**, https://doi.org/10.1002/anie.201707584; *Angew. Chem.* **2017**, https://doi.org/10.1002/ange.201707584.

[3] a) E. J. Horn, B. R. Rosen, Y. Chen, J. Tang, K. Chen, M. D. Eastgate, P. S. Baran, *Nature* **2016**, *533*, 77–81; b) R. Hayashi, A. Shimizu, J. Yoshida, *J. Am. Chem. Soc.* **2016**, *138*, 8400–8403; c) L. Schulz, M. Enders, B. Elsler, D. Schollmeyer, K. M. Dyballa, R. Franke, S. R. Waldvogel, *Angew. Chem. Int. Ed.* **2017**, *56*, 4877–4881; *Angew. Chem.* **2017**, *129*, 4955–4959; d) N. Fu, G. S. Sauer, A. Saha, A. Loo, S. Lin, *Science* **2017**, *357*, 575–579; e) R. Feng, J. A. Smith, K. D. Moeller, *Acc. Chem. Res.* **2017**, *50*, 2346–2352.

[4] a) J. Yoshida, *Electrochem. Soc. Interface* **2009**, 40–45; b) K. Watts, A. Baker, T. Wirth, *J. Flow Chem.* **2014**, *4*, 2–11; c) A. Folgueiras-Amador, T. Wirth, *J. Flow Chem.* **2017**, https://doi.org/10.1556/1846.2017.00020; d) M. Atobe, H. Tateno, Y. Matsumura, *Chem. Rev.* **2017**, https://doi.org/10.1021/acs.chemrev.7b00353.

[5] S. J. Yoo, L.-J. Li, C.-C. Zeng, R. D. Little, *Angew. Chem. Int. Ed.* **2015**, *54*, 3744–3747; *Angew. Chem.* **2015**, *127*, 3815–3818.

[6] a) D. Horii, M. Atobe, T. Fuchigami, F. Marken, *Electrochem. Commun.* **2005**, *7*, 35–39; b) R. Horcajada, M. Okajima, S. Suga, J. Yoshida, *Chem. Commun.* **2005**, 1303–1305; c) P. He, P. Watts, F. Marken, S. J. Haswell, *Angew. Chem. Int. Ed.* **2006**, *45*, 4146–4149; *Angew. Chem.* **2006**, *118*, 4252–4255; d) J. Kuleshova, J. T. Hill-Cousins, P. R. Birkin, R. C. D. Brown, D. Pletcher, T. J. Underwood, *Electrochim. Acta* **2011**, *56*, 4322–4326; e) A. Attour, P. Dirrenberger, S. Rode, A. Ziogas, M. Matlosz, F. Lapicque, *Chem. Eng. Sci.* **2011**, *66*, 480–489; f) T. Kashiwagi, B. Elsler, S. R. Waldvogel, T. Fuchigami, M. Atobe, *J. Electrochem. Soc.* **2013**, *160*, G3058–G3061; g) M. A. Kabeshov, B. Musio, P. R. D. Murray, D. L. Browne, S. V. Ley, *Org. Lett.* **2014**, *16*, 4618–4621; h) M. R. Chapman, Y. M. Shafi, N. Kapur, B. N. Nguyen, C. E. Willans, *Chem. Commun.* **2015**, *51*, 1282–1284; i) R. A. Green, R. C. D. Brown, D. Pletcher, B. Harji, *Org. Process Res. Dev.* **2015**, *19*, 1424–1427; j) C. Gütz, M. Bänziger, C. Bucher, T. R. Galvão, S. R. Waldvogel, *Org. Process Res. Dev.* **2015**, *19*, 1428–1433; k) R. A. Green, D. Pletcher, S. G. Leach, R. C. D. Brown, *Org. Lett.* **2015**, *17*, 3290–3293; l) R. A. Green, R. C. D. Brown, D. Pletcher, B. Harji, *Electrochem. Commun.* **2016**, *73*, 63–66; m) C. Gütz, A. Stenglein, S. R. Waldvogel, *Org. Process Res. Dev.* **2017**, *21*, 771–778.

[7] a) K. Watts, W. Gattrell, T. Wirth, *Beilstein J. Org. Chem.* **2011**, *7*, 1108–1114; b) K. Arai, K. Watts, T. Wirth, *ChemistryOpen* **2014**, *3*, 23–28; c) K. Arai, T. Wirth, *Org. Process Res. Dev.* **2014**, *18*, 1377–1381.

[8] a) T. J. Donohoe, C. K. A. Callens, A. Flores, A. R. Lacy, *Chem. Eur. J.* **2011**, *17*, 58–76; b) P. H. Fuller, J. Kim, S. R. Chemler, *J. Am. Chem. Soc.* **2008**, *130*, 17638–17639; c) G. Yang, W. Zhang, *Org. Lett.* **2012**, *14*, 268–271.

[9] a) H. C. Xu, J. M. Campbell, K. D. Moeller, *J. Org. Chem.* **2014**, *79*, 379–391; b) F. Xu, L. Zhu, S. Zhu, X. Yan, H. C. Xu, *Chem. Eur. J.* **2014**, *20*, 12740–12744; c) L. Zhu, P. Xiong, Z. Y. Mao, Y. H. Wang, X. Yan, X. Lu, H. C. Xu, *Angew. Chem. Int. Ed.* **2016**, *55*, 2226–2229; *Angew. Chem.* **2016**, *128*, 2266–2269; d) Z. W. Hou, Z. Y. Mao, H. B. Zhao, Y. Y. Melcamu, X. Lu, J. Song, H. C. Xu, *Angew. Chem. Int. Ed.* **2016**, *55*, 9168–9172; *Angew. Chem.* **2016**, *128*, 9314–9318; e) P. Xiong, H. H. Xu, H. C. Xu, *J. Am. Chem. Soc.* **2017**, *139*, 2956–2959.

[10] E. W. Washburn, *International Critical Tables of Numerical Data, Physics, Chemistry and Technology*, National Academy of Sciences, McGraw Hill, New York, **1926**.

[11] a) L. Eberson, O. Persson, M. P. Hartshorn, *Angew. Chem. Int. Ed. Engl.* **1995**, *34*, 2268–2269; *Angew. Chem.* **1995**, *107*, 2417–2418; b) L. Eberson, M. P. Hartshorn, O. Persson, *J. Chem. Soc. Perkin Trans. 2* **1995**, 1735–1744.

[12] H. C. Xu, K. D. Moeller, *J. Am. Chem. Soc.* **2010**, *132*, 2839–2844.

[13] J. M. Campbell, H. C. Xu, K. D. Moeller, *J. Am. Chem. Soc.* **2012**, *134*, 18338–18344.

[14] R. Manoharan, M. Jeganmohan, *Chem. Commun.* **2015**, *51*, 2929–2932.

[15] CCDC 1569516 (**12**), 1569515 (**23a**) and 1569517 (**23b**) contain the supplementary crystallographic data for this paper. These data can be obtained free of charge from The Cambridge Crystallographic Data Centre.

[16] J. Gui, H. Tian, W. Tian, *Org. Lett.* **2013**, *15*, 4802–4805.

[17] The Zn cartridge was prepared using silica as the support (60–100 mesh, 50% in weight). This was required to reduce the backpressure produced due to the small size of the Zn dust particles ($< 10\ \mu m$).

[18] a) P. G. M. Wuts, Y. W. Jung, *J. Org. Chem.* **1988**, *53*, 1957–1965; b) D. A. Dias, M. A. Kerr, *Org. Lett.* **2009**, *11*, 3694–3697.

[19] X.-Y. Qian, S.-Q. Li, J. Song, H.-C. Xu, *ACS Catal.* **2017**, *7*, 2730–2734.

[20] a) R. A. Green, D. Pletcher, S. G. Leach, R. C. D. Brown, *Org. Lett.* **2016**, *18*, 1198–1201; b) R. Stalder, G. P. Roth, *ACS Med. Chem. Lett.* **2013**, *4*, 1119–1123.

Manuscript received: September 19, 2017
Accepted manuscript online: October 17, 2017
Version of record online: November 2, 2017

